Etched and non-etched polystyrene nanoballs coated with AuNPs on Indium Tin Oxide (ITO) electrode as H_2O_2 sensor

IOP Conf. Series: Earth and Environmental Science **277** (2019) 012032 doi:10.1088/1755-1315/277/1/012032

Etched and non-etched polystyrene nanoballs coated with AuNPs on Indium Tin Oxide (ITO) electrode as H_2O_2 sensor

G M A Saputra[1], A Purwidyantri[2], C-M Yang[3,4,5], B A Prabowo[3,6,*] and C-S Lai[3,7,8,]**

[1] Boyolangu 1 State High School, Tulungagung, Indonesia
[2] Research Unit for Clean Technology, Indonesian Institute of Sciences, Bandung, Indonesia
[3] Department of Electronic Engineering, Chang Gung University, Taoyuan, Taiwan
[4] Institute of Electro-Optical Engineering, Chang Gung University, Taoyuan, Taiwan
[5] Department of General Surgery, Chang Gung Memorial Hospital, Taoyuan, Taiwan
[6] Research Center for Electronics and Telecommunications, Indonesian Institute of Sciences, Bandung, Indonesia
[7] Department of Nephrology, Chang Gung Memorial Hospital, Taoyuan, Taiwan
[8] Department of Materials Engineering, Ming-Chi University of Technology, New Taipei City, Taiwan

E-mail: *briliant.adhi.prabowo@lipi.go.id, **cslai@mail.cgu.edu.tw

Abstract. In electro-analytical applications, metallic nanoparticles (NPs) facilitate roughening of the conductive sensing interface and electrochemical signal amplification as a result of some metal NPs catalytic properties. In this study, natural lithography, termed as nanospheres lithography (NSL), was used to fabricate 5 nm thick AuNPs from thermal evaporation system on an Indium Tin Oxide (ITO) substrate patterned with polystyrene (PS) nanoballs (d=100 nm). The electrode substrate was characterized by field-emission scanning electron microscopy (FE-SEM), energy-dispersive X-ray spectroscopy (EDX), and cyclic voltammetry (CV) and utilized as a sensor to measure H_2O_2. More prominent features were shown by the etched PS on the fabricated electrode that left AuNPs honeycomb-like pattern than the non-etched one. Higher oxidation peak was demonstrated by the etched electrode than non-etched electrode as recorded with cyclic voltammogram, as well as in H_2O_2 measurement. CV outcomes denoted higher surface area at the substrate with etched PS and resulted in a lower limit of detection (LOD) of H_2O_2 than the non-etched substrates.

1. Introduction

In electro-analytical applications, metal nanoparticles (NPs) offer the potency in roughening of the conductive sensing interface and electrochemical signal amplification as a result of their catalytic properties. At nanoscale dimensions, metal NPs have conductivity properties allowing the electrical contact among protein's redox centers with the electrode surfaces. Besides, noble metal NPs are broadly used in biomedical, environmental, industrial, electronics, photonics, catalysts, and biotechnology [1–6]. These metal NPs generate high surface area, nontoxicity, excellent biocompatibility, chemical stability, and also show fast electron transfer when modified with an electrode which is essential in electro-analytic applications [7,8].

AuNPs offer unique properties for biosensor constructions because they provide a suitable microenvironment. AuNPs also exhibit excellent conducting capability and high surface-to-volume ratio which make them significantly distinguished from the non-nano gold particle. It is remarkably noted that AuNPs are a good catalyst for reduction and oxidation of hydrogen peroxide (H_2O_2), whereas, gold electrode is a poor catalyst for it [7].

One of the general techniques used at a clean room for AuNPs fabrication is photolithography. However, photolithography is an expensive technique for nanomaterial fabrication. Photolithography is also laborious and requires advanced instrumentations. In this study, nanosphere lithography (NSL) was applied to facilitate a simple and cost-effective nanostructuring technique which can be downscaled and tuned easily. Nanosphere lithography (NSL) in this work refers to nanoporous material fabrication using a cost-efficient synthesis procedure that generates noble metal nanoparticle arrays patterns in a large area providing both top-down and bottom-up techniques [8,9]. There are numerous colloidal spheres used as porous nanomaterial templates to produce two-dimensional (2D) arrangement and three-dimensional (3D) colloidal crystals, such as polystyrene (PS), silica, and latex beads. Nanopatterning can easily be conducted using this technique with simple, inexpensive and an inherently parallel fabrication of a functionalization process. Moreover, the NSL remarkable features also emphasize the ease of replication and high monodispersity of the nanostructures assembled for a single or batched sample preparation. In this study, the patterned electrode was applied as a hydrogen peroxide sensor in an electrochemical setup. The impact of the surface area towards the redox reaction onto interface is highlighted.

Hydrogen peroxide (H_2O_2) is an example of strong oxygen donors and also a reactive oxygen species which is toxic for living creature. It affects cellular mechanisms and induces oxidative damage which results in cell death [10]. It is known as one of the respiration by-products, an end product of metabolic reactions, particularly peroxisomal oxidation pathways, and a likely transmitter of cellular signals [11–13]. Therefore, the measurement of H_2O_2 is important as one of the health screening parameters.

In the current work, a simple fabrication of nanopatterned and downscaled AuNPs on ITO electrode for electrochemical H_2O_2 sensor with the higher surface area is presented. The templating with small size of polystyrene (PS) nanoballs had been proven effective in providing a highly regular template as well as the ease of etching process for nanopatterning.

2. Materials and methods

2.1. Materials

Standard H_2O_2 was purchased from Merck (Germany). PS nanoballs with diameter 100 nm and phosphate buffer saline (PBS) were purchased from Sigma Aldrich (St. Louis, MO, USA). Whereas toluene, acetone, isopropyl alcohol (IPA) were purchased from Avantor (Pennsylvania, USA). ITO on the glass substrate (thickness 0.7 mm with sheet resistance 7 Ω/square) was purchased from Uni-Onward (Taipei, Taiwan). Potassium chloride and sodium dodecyl sulfate were purchased from Merck (Darmstadt, Germany). Gold evaporation slug was purchased from Sigma Aldrich (St. Louis, MO, USA). Deionized water that used for this research (resistivity in 25°C = 18.2 MΩ•cm) obtained through Milli-Q system.

2.2. Assembly of the AuNP on an ITO electrode and surface modification

For preparation, the ITO substrate was washed first and dried with N_2. Polystyrene (PS) nanoballs with a diameter of 100 nm was drop-casted onto the ITO substrate following methods mentioned elsewhere after ITO's hydrophilicity was acquired [8]. The substrates were dried at three successive conditions to get the monolayer nanoballs: first at room temperature, then in an 80°C incubator and last on a 100°C hot plate. The substrate coated with polystyrene nanoballs on their surfaces was transferred into a thermal evaporation chamber to deposit Au film with a thickness of 5 nm. The system setup was 1 Å/s for deposition rate with pressure under 10^6 mTorr. To get AuNPs with nanoring structure (the etched treatment), the polystyrene nanoballs were etched using toluene.

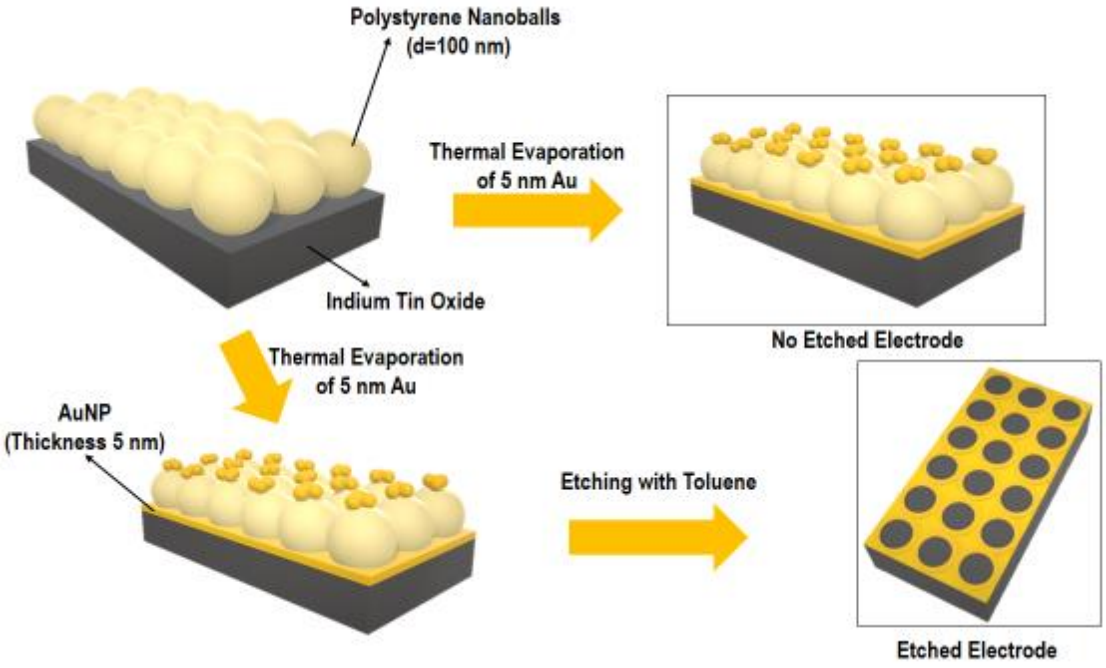

Figure 1. AuNPs coating on ITO electrode fabrication flow with two combinations of the nanostructure, without PS etching and with PS etching.

2.3. Surface investigation of ITO electrode

The fabricated electrodes were investigated using FE-SEM and EDX for morphological observation and cyclic voltammetry (CV), respectively. To confirm the enhancement of AuNPs on electrochemical signal amplification, CV was conducted at various scan rate using 5×10^{-6} mol/cm^3 $K_3[Fe(CN)_6]/K_4[Fe(CN)_6]$ and 0.5 M KCl solution.

2.4. Investigation of the stability and sensing performance of the fabricated electrodes

Potentiostat with 3 electrode system was used: Ag/AgCl as a reference electrode, Pt as a counter electrode, and ITO coated AuNPs as a working electrode. The stability of the fabricated electrode was checked by CV technique performed with the potential between -0.1 to 0.6 V. Standard solution for CV test was 5×10^{-6} mol/cm^3 $K_3[Fe(CN)_6]$ and 0.5 M KCl. After CV stability at various scan rates were achieved, H_2O_2 sensing was conducted using the fabricated electrode using CV taken at the scan rate of 100 mV/s.

3. Result and discussion

3.1. Electrode surface characterization

Figure 2a shows the morphology of the AuNPs growth through thermal evaporation. The self-assembly drop coating of the nanoballs in NSL method has resulted in high uniformity and density of the particles. In Figure 2b, PS nanoballs (d=100 nm) coated with AuNPs and left without etching treatment were portrayed and affirmed the presence of Au in cyclic voltammogram as well as recorded by EDX (Figure 2d). In Figure 2c, it is clearly observed that the PS etching treatment group successfully grew a highly periodic Au-nanoring pattern. Besides, a considerably high amount of Au element was captured by EDX (Figure 2e).

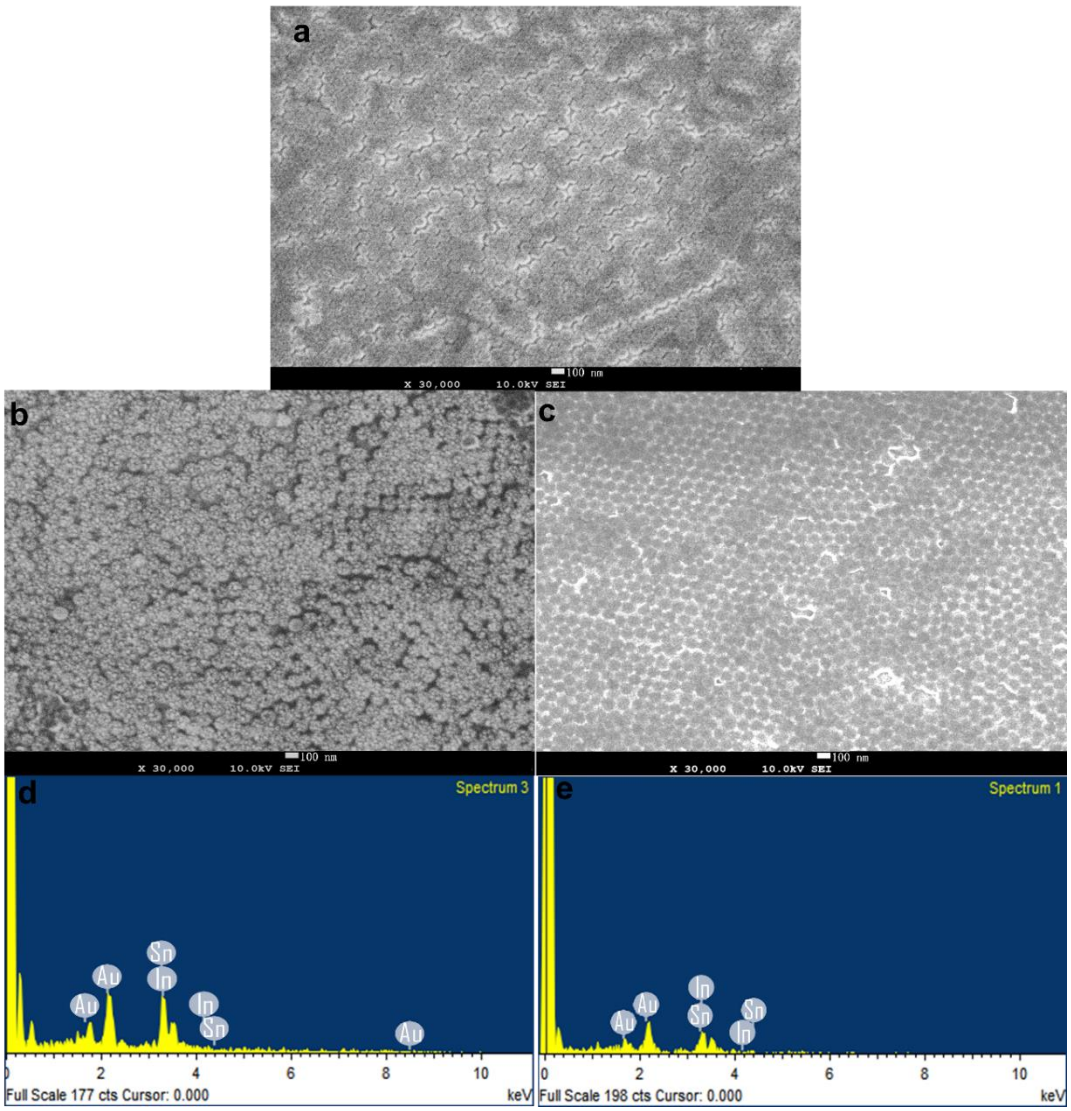

Figure 2. FE-SEM figures of ITO electrode coated with (a) PS nanoballs, (b) AuNPs without PS etching and (c) AuNPs after PS etching treatments. EDX Figures of ITO electrode coated with PS nanoballs and (d) AuNPs without PS etching, (e) AuNPs with PS etching.

3.2. Stability and sensing performance of the fabricated electrodes

Figure 3a and b display the cyclic voltammogram stability of the non-etched and etched electrode, respectively. A positive correlation between scan rates with current peak was apparently seen. The higher redox reaction on the interface was likely to occur in the etched electrode as shown in the larger CV curve range. The oxidation and reduction peak trends of the fabricated electrodes were plotted and compared in Figure 3c and d. The reduction and oxidation peaks of the etched fabricated electrode were approximately 28% higher than the non-etched electrode as being quantified from the slope produced by the anodic peak current plots. The cyclic voltammogram of non-etched fabricated electrode showed reduction current peak of -18.82 μA and oxidation current peak of 13.16 μA for scan rate 100 mV/s (Figure 3c), while etched fabricated electrode showed a reduction current peak of -19.95 μA and an oxidation peak of 13.99 μA for the same scan rate (Figure 3d), which was higher than the non-etched electrode.

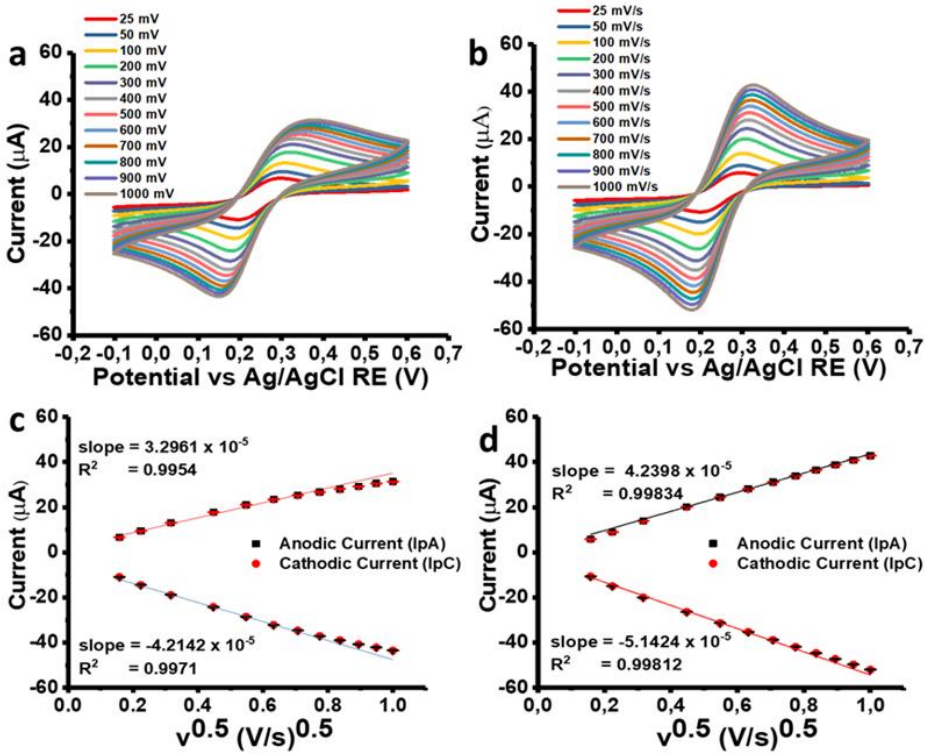

Figure 3. CV measurements recorded from the redox measurement of 5 mM $K_3[Fe(CN)_6]/K_4[Fe(CN)_6]$ and 0.5 M KCl at various scan rates for (a) non-etched and (b) etched fabricated electrodes, and the relation curves of the anodic peak current on the scan rate square root with the calculated correlation coefficient rates for (c) non-etched and (d) etched electrodes.

Subsequently, the Randles-Sevcik equation was used to calculate the electroactive surface area of the etched fabricated electrode [14,15]:

$$i_p = 2.686\ x\ 10^5 n^{3/2} A c D^{1/2} v^{1/2}$$

where i_p is the peak current in amperes, A is the electrode area in cm^2, D is the diffusion coefficient in cm^2/s, c is the concentration in mol/cm^3, and v is the scan rate in V/s. Using this equation, the electroactive surface area of the etched fabricated electrode was calculated to be around 0.03 cm^2, while the non-etched electrode only showed about 0.009 cm^2 electro-active area. The electro-active surface area is dependent on the nanostructure morphology and can be varied from one to other methods of sensing membrane fabrication.

After CV stability evaluation, the fabricated electrodes were then used to measure H_2O_2 in PBS solution with a scan rate of 100 mV/s. A series of H_2O_2 concentration from 10 μM to 5×10^4 μM H_2O_2 was applied throughout the present work. In order to demonstrate the ability of the proposed device on measuring a wide dynamic range, the increment of the response signal was recorded as the logarithmic scale of the H_2O_2 concentration in μM (Figure 4) [16].

Figure 4a and 4c showed that the fabricated sensors excellently responded to the increasing concentration of H_2O_2 as seen in the cyclic voltammograms. As shown in Figure 4c and 4d, the etched electrode (Figure 4d) exhibited a more significant increment of redox current peaks than the non-etched electrode (Figure 4c). For instance, at 5×10^4 μM, the etched electrode oxidation peak was 0.277 μA (Figure 4c), while the non-etched electrode peak was about 0.258 μA (Figure 4a). As depicted in Figure 4d, the etched fabricated electrode initially produced a small slope which was gradually increased near the reduction or oxidation peak. This was plausible since the electro-active surface area of the etched surface was wider and required more time to distribute the electric current evenly on the interface.

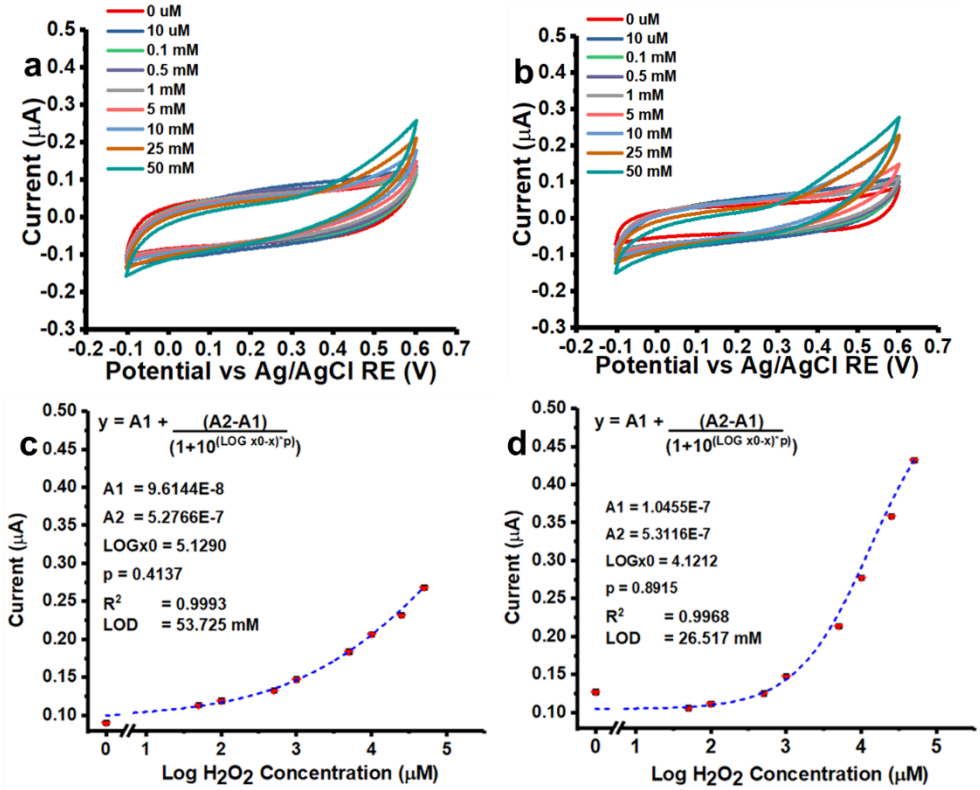

Figure 4. H_2O_2 electrochemical sensing performances using (a) non-etched and (b) etched electrodes. The sensing response curves of different H_2O_2 concentration measurement using (c) non-etched and (d) etched electrodes.

The limitation of detection (LOD) was determined from the minimum H_2O_2 concentration which caused the change in current signal response equivalent to three times the average background noise in the absence of H_2O_2 solution [16]. As a result, the detection limit of the non-etched and the etched fabricated electrode was 53.725 mM and 26.517 mM, respectively.

4. Conclusion

In this study, an electrochemical sensor with etched and non-etched PS nanoballs to enhance electrochemical signal for H_2O_2 sensor was designed. The etched electrode shows a higher electrochemical redox signal than the non-etched electrode represented in cyclic voltammograms. In a future outlook, a lower concentration of H_2O_2 can be targeted and measured in more stable buffer with real-time experimental setup.

Acknowledgments

Parts of this study was presented in the 2018 Indonesian Youth Science Competition *(Lomba Karya Ilmiah Remaja/LKIR 2018)*. The authors wholeheartedly thank Chang Gung Memorial Hospital (CGMH) Taiwan, for part of financial support under the contract number CMRPD2G0102; Ministry of Science and Technology (MOST) Taiwan under the contract number MOST 107-2911-I-182-502 and MOST 107-2218-E-182-006; Kurita Water and Environment Foundation (KWEF) Japan and Asian Institute of Technology (AIT) Thailand for Kurita-AIT Research Grant 2018; and the Indonesian Institute of Sciences (LIPI).

References

[1] Zhu C, Du D, Eychmu A and Lin Y 2015 *Chem. Rev.* **115** 8896–943
[2] Dauthal P and Mukhopadhyay M 2016 *Ind. Eng. Chem. Res.* **55** 9557–77

[3] Han J, Wang M, Hu Y, Zhou C and Guo R 2017 *Prog. Polym. Sci.* **70** 52–91
[4] Rai M, Ingle A P, Birla S, Yadav A, Alves C and Santos D 2016 *Crit. Rev. Microbiol.* **42** 696–719
[5] Liu W, Herrmann A, Bigall N C, Rodriguez P, Wen D, Oezaslan M, Schmidt T J, Gaponik N, and Eychmüller A 2014 *Acc. Chem. Res.* **48** 154–62
[6] Rai M, Ingle A P, Gupta I and Brandelli A 2015 *Int. J. Pharm.* **496** 159–72
[7] Viswanathan S and Manisankar P 2015 *J. Nanosci. Nanotechnol.* **15** 6914–23
[8] Purwidyantri A, Chen C H, Hwang B J, Luo J D, Chiou C C, Tian Y C, Lin C Y, Cheng C H, Lai C S 2016 *Biosens. Bioelectron.* **77** 1086–94
[9] Purwidyantri A, El-Mekki I and Lai C S 2017 *IEEE Trans. Nanotechnol.* **16** 551–9
[10] Yoona J, Lee T, Bapurao B, Jo J, Oh B K and Choi J W 2017 *Biosens. Bioelectron.* **93** 14–20
[11] Zorov D B, Juhaszova M and Sollott S J 2014 *Physiol. Rev.* **94** 909–50
[12] Fransen M, Lismont C and Walton P 2017 *Int. J. Mol. Sci.* **18** 1126
[13] Lodhi I J and Semenkovich C F *Cell Metab.* **19** 380–92
[14] Shabani-Nooshabadi M, Roostaee M and Karimi-Maleh H 2017 *J. Iran. Chem. Soc.* **14** 955–61
[15] Ramanathan M, Patil M, Epur R, Yun Y, Shanov V, Schulz M, Heineman W R, Datta M K and Kumta P N 2016 *Biosens. Bioelectron.* **77** 580–8
[16] Purwidyantri A, Kamajaya L, Chen C H, Luo J D, Chiou C C, Tian Y C, Lin C Y, Yang C M and Lai C S 2018 *J. Electrochem. Soc.* **165** 3170–7